

Synthesis and Crystal Structure of Two New Discrete, Neutral Complexes of Manganese and Zinc Using a Rigid Organic Clip

Partha Sarathi Mukherjee,* Kil Sik Min, Atta M. Arif, and Peter J. Stang*

Department of Chemistry, University of Utah, 315 South 1400 East, Room 2020, Salt Lake City, Utah 84112

Received May 27, 2004

Two discrete neutral dimanganese(II) and tetrazinc(II) complexes were synthesized from a rigid organic clip and the corresponding metal acetates. The compounds were characterized by elemental analysis and single crystal X-ray diffraction study. The manganese species is a dinuclear discrete product with two disordered acetates bridging two manganese centers, while the zinc one consists of two octahedral and two tetrahedral Zn(II) centers with both bridging acetates and triply μ_3 -hydroxides. Variable temperature magnetic measurement reveals the existence of weak antiferromagnetic interaction ($J = -1.6 \text{ cm}^{-1}$; $H = -2JS_1 \cdot S_2$) within the manganese complex.

Introduction

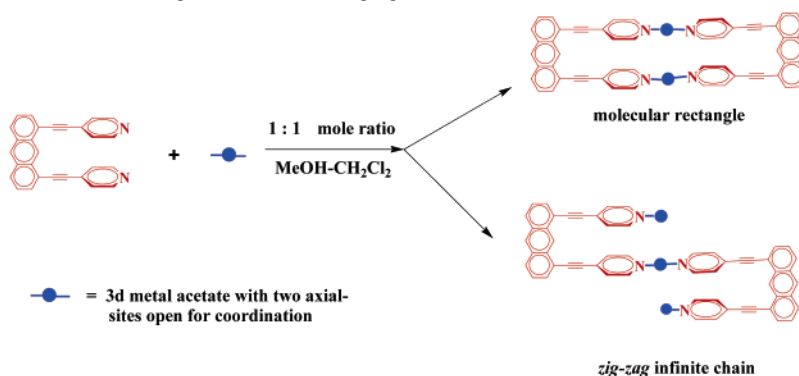
Coordination-driven self-assembly of discrete molecular ensembles is a growing area at the forefront of modern supramolecular chemistry.¹ Metallomacrocycles are an important class of compounds in this field. For the design of metallomacrocycles, one must take into account the shape, rigidity, number, and disposition of coordination sites of the donor organic ligand as well as oxidation state, geometry, and coordination number of the metal center. Up to now, the most frequently prepared species were those having high symmetry, for example, two-dimensional polygonal macrocycles such as molecular triangles, squares, pentagons, and hexagons.² In comparison, relatively simple and lower-symmetry species such as 2D rectangular-shaped molecular structures have remained rare.^{3a–b}

A majority of the metallomacrocycles reported to date are based on Pt(II) and Pd(II) using nitrogen donor neutral ligands, and thus, the resulting assemblies are ionic.^{1a,3} A few neutral assemblies have also been reported. These species

* To whom correspondence should be addressed. E-mail: stang@chem.utah.edu (P.J.S.); part_dip@hotmail.com (P.S.M.).

- (1) (a) Seidel, S. R.; Stang, P. J. *Acc. Chem. Res.* **2002**, *35*, 972. (b) Swiegers, G. F.; Malefetse, T. J. *Coord. Chem. Rev.* **2002**, *225*, 91. (c) Holliday, B. J.; Mirkin, C. A. *Angew. Chem., Int. Ed.* **2001**, *40*, 2022. (d) Cotton, F. A.; Lin, C.; Murillo, C. A. *Acc. Chem. Res.* **2001**, *34*, 759. (e) Fujita, M.; Umemoto, K.; Yoshizawa, M.; Fujita, N.; Kusakawa, T.; Biradha, K. *Chem. Commun.* **2001**, 509. (f) Leininger, S.; Olenyuk, B.; Stang, P. J. *Chem. Rev.* **2000**, *100*, 853. (g) Fujita, M. *Chem. Soc. Rev.* **1998**, *27*, 417. (h) Uller, E.; Demleitner, I.; Bernt, I.; Saalfrank, R. W. Synergistic Effect of Serendipity and Rational Design in Supramolecular Chemistry. In *Structure and Bonding*; Fujita, M., Ed.; Springer: Berlin, 2000; Vol. 96, p 149. (i) Caulder, D. L.; Raymond, K. N. *Acc. Chem. Res.* **1999**, *32*, 975. (j) Baxter, P. N. W.; Lehn, J.-M.; Baum, G.; Fenske, D. *Chem. Eur. J.* **1999**, *5*, 102. (k) Chambon, J.-C.; Dietrich-Buchecker, C.; Sauvage, J.-P. Transition Metals as Assembling and Templating Species. In *Comprehensive Supramolecular Chemistry*; Lehn, J.-M., Chair, E., Atwood, J. L., Davis, J. E. D., MacNicol, D. D., Vogtle, F., Eds.; Pergamon Press: Oxford, 1996; Vol. 9, Chapter 2, p 43. (l) Lehn, J.-M. *Supramolecular Chemistry: Concepts and Perspectives*; VCH: New York, 1995.
- (2) (a) Kryshchenko, Y. K.; Seidel, S. R.; Arif, A. M.; Stang, P. J. *J. Am. Chem. Soc.* **2003**, *125*, 5193. (b) Qin, Z.; Jennings, M. C.; Puddephatt, R. J. *Inorg. Chem.* **2002**, *41*, 3967. (c) Pak, J. J.; Greaves, J.; McCord, D. J.; Shea, K. J. *Organometallics* **2002**, *21*, 3552. (d) Lee, S. J.; Lin, W. *J. Am. Chem. Soc.* **2002**, *124*, 4554. (e) Liu, X.; Stern, C. L.; Mirkin, C. A. *Organometallics* **2002**, *21*, 1017. (f) Han, G.; Dong, G.; Duan, C.-Y.; Mo, H.; Meng, Q.-J. *New J. Chem.* **2002**, *26*, 1371. (g) Sun, S.-S.; Anspach, J. A.; Lees, A. J. *Inorg. Chem.* **2002**, *41*, 1862. (h) Cotton, F. A.; Lin, C.; Murillo, C. A. *J. Am. Chem. Soc.* **2001**, *123*, 2670. (i) Cotton, F. A.; Daniels, L. M.; Lin, C.; Murillo, C. A.; Yu, S.-Y. *J. Chem. Soc., Dalton Trans.* **2001**, 502. (j) Manimaran, B.; Thanasekaran, P.; Rajendran, T.; Lin, R.-J.; Chang, I.-J.; Lee, G.-H.; Peng, S.-M.; Rajagopal, S.; Lu, K.-L. *Inorg. Chem.* **2002**, *41*, 5323. (k) Cui, Y.; Ngo, H. L.; Lin, W. *Inorg. Chem.* **2002**, *41*, 1033. (l) Schmitz, M.; Leininger, S.; Fan, J.; Arif, A. M.; Stang, P. J. *Organometallics* **1999**, *18*, 4817. (m) Habicher, T.; Nierengarten, J.-F.; Gramlich, V.; Diederich, F. *Angew. Chem., Int. Ed.* **1998**, *37*, 1916. (n) Hartshorn, C. M.; Steel, P. J. *Inorg. Chem.* **1996**, *35*, 6902. (o) Abourahma, H.; Moulton, B.; Kravtsov, V.; Zaworotko, M. J. *J. Am. Chem. Soc.* **2002**, *124*, 9990. (p) Campos-Fernández, C. S.; Clérac, R.; Koomen, J. M.; Russell, D. H.; Dunbar, K. R. *J. Am. Chem. Soc.* **2001**, *123*, 773. (q) Stang, P. J.; Persky, N. E.; Manna, J. J. *Am. Chem. Soc.* **1997**, *119*, 4777.
- (3) (a) Kuehl, C. J.; Huang, S. D.; Stang, P. J. *J. Am. Chem. Soc.* **2001**, *123*, 9634. (b) Kuehl, C. J.; Mayne, C. L.; Arif, A. M.; Stang, P. J. *Org. Lett.* **2000**, *2*, 3727. (c) Su, C.-Y.; Cai, Y.-P.; Chen, C.-L.; Smith, M. D.; Kaim, W.; Loye, H.-C. *J. Am. Chem. Soc.* **2003**, *125*, 8595. (d) Grosshans, P.; Jouaiti, A.; Bulach, V.; Planeix, J.-M.; Hosseini, M. W.; Kyritsakas, N. *Eur. J. Inorg. Chem.* **2004**, 453 and references therein.
- (4) Cotton, F. A.; Donahue, J. P.; Murillo, C. A. *J. Am. Chem. Soc.* **2003**, *125*, 5436. (b) Cotton, F. A.; Lin, C.; Murillo, C. A. *Inorg. Chem.* **2001**, *40*, 478. (c) Cotton, F. A.; Lin, C.; Murillo, C. A. *Inorg. Chem.* **2001**, *40*, 6413. (d) Cheng, H.; Chun-Ying, D.; Chen-jie, F.; Yong-jiang, L.; Qing-jin, M. *J. Chem. Soc., Dalton Trans.* **2000**, 1207. (e) Cotton, F. A.; Daniels, L. M.; Lin, C.; Murillo, C. A. *J. Am. Chem. Soc.* **1999**, *121*, 4538.

Scheme 1. Self-Assembly of Molecular Rectangle and/or Infinite Zigzag Chain



are based upon coordination of anionic ligands to Mo,⁴ Rh,⁵ Re,⁶ and Pt.⁷

Discrete, finite assemblies of 3d-series metal ions are particularly appealing because of the potential of incorporating a variety of desirable magnetic, electronic, optical, and catalytic properties.^{3c,d} The coordination sphere of these metals is flexible, and thus, the geometry of the final assemblies is less predictable. In the majority of cases, the products of the reaction of these metal ions with organic bridging ligands are polymeric in nature.⁸

Here, in the continuation of our investigation on the chemistry of discrete molecular systems, we describe the formation of two new neutral dimanganese (**3a**) and tetrazinc (**3b**) discrete assemblies using a rigid organic clip and metal acetate as building blocks.

Result and Discussion

The synthetic strategy known as the “directional bonding approach” for molecular architectures is well established.^{9,1a-d} We have already demonstrated the formation of molecular rectangles using a diplatinum clip in combination with linear nitrogen or oxygen donor organic bridging ligands.^{3,7} To investigate the complementary approach to the previous strategy, we have selected 1,8-bis(4-pyridylethynyl)anthracene as a rigid organic clip (**1**) in combination with the axially accessible 3d-metal acetate (**2**) as linear linker. In principle, an equimolar combination of **1** and **2** can lead to the formation of either dimeric rectangular species or zigzag polymeric chains as shown in Scheme 1.

Mn(II), Zn(II), and Cu(II) acetates were reacted with ligand **1** in an equimolar ratio. The former one resulted in the formation of a dimanganese rectangular product (**3a**) with a weak bridging acetate while Zn(II) acetate produced an unusual tetrazinc discrete product (**3b**) with both tetrahedral and octahedral zinc centers (Scheme 2). In contrast, the similar reaction using Cu(II) acetate yielded a deep green product (**4**) which was insoluble in all common organic solvents, possibly due to the formation of polymeric product. The composition and shape of **3a** and **3b** were established by elemental analyses and X-ray single crystal structure determination. Attempts to obtain single crystals of the Cu(II) analogue (**4**) were unsuccessful due to its insolubility in common solvents.

Crystal Structure of Complex 3a. X-ray crystallography unambiguously established the structure of **3a**, a discrete neutral rectangular molecule. The structure consists of a dimanganese $\text{Mn}_2(\mu\text{-OAc})_2(\text{OAc})_2$ motif and two organic clips per formula unit as shown in Figure 1. Crystallographic data and other parameters are given in Table 1. Two ligands are arranged in a face-to-face conformation to coordinate two Mn(II) ions from opposite directions through axial positions, generating a locally pseudo-octahedral geometry around the metals. The equatorial sites of each Mn(II) are occupied by acetate oxygen. Two disordered acetates bridge both the Mn(II) centers by weak bonding interaction, while the other two basal sites of each Mn(II) are coordinated by a bidentate chelating acetate. Selected bond parameters around the coordination sphere of each Mn(II) are given in Table 2. The overall length of **3a** is 18.1 Å. The width, as defined by the intramolecular Mn–Mn distance, is 4.1 Å while the C(8)–C(18) distance is 4.97 Å. The larger C–C separation indicates that the clip is compressed and creating potential strain in the structure. The bridging acetate affects the geometry of **3a** such that the manganese ions are forced to bend inward, which in turn causes the rectangle to appear relatively narrowed in the middle. The bending is due to the bridging nature of the acetate which pulls the manganese atoms closer. The pyridine rings of each bridging ligand **1** are almost perpendicular. The distance between the centroid of one pyridine and closest H–C hydrogen of the perpendicular pyridine is 3.0 Å, resulting in a C–H– π supramolecular interaction. The packing diagram of **3a** (Figure 2) reveals the formation of a channel along the crystallographic

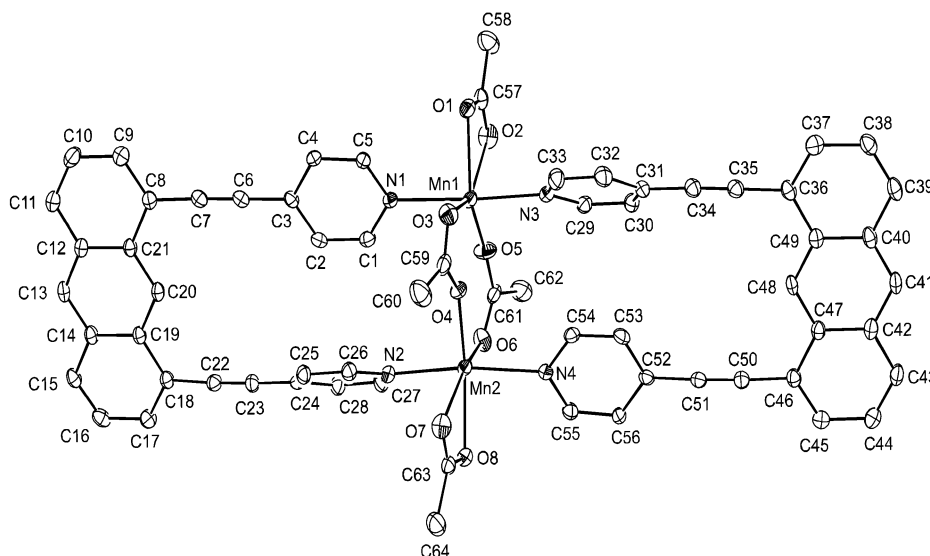
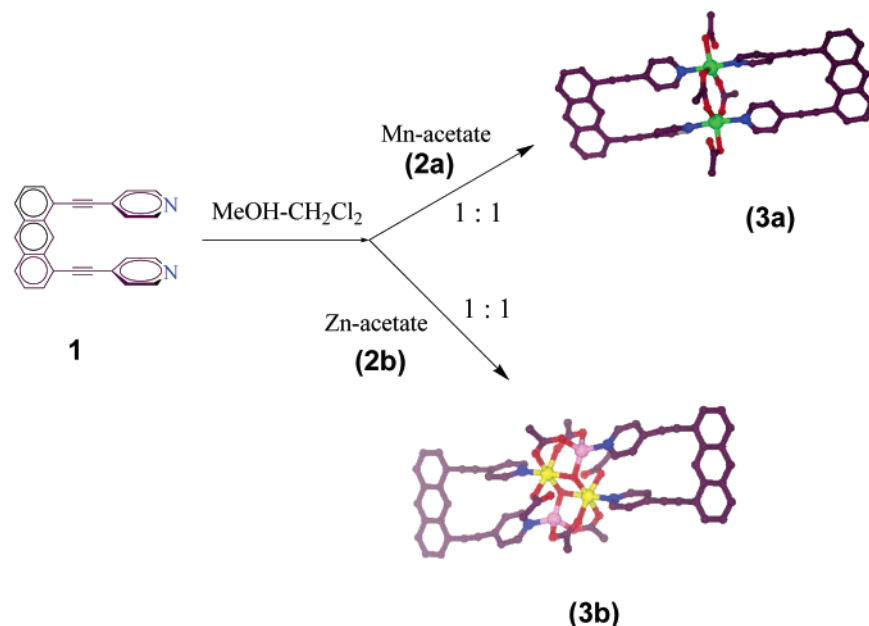
(5) Cotton, F. A.; Lin, C.; Daniels, M. L.; Murillo, C. A.; Yu, S.-Y. *J. Chem. Soc., Dalton Trans.* **2001**, 502.

(6) (a) Bala, M.; Thanasekaran, P.; Rajendran, T.; Liao, R. T.; Liu, Y. H.; Lee, G. H.; Peng, S. M.; Rajagopal, S.; Lu, K. L. *Inorg. Chem.* **2003**, *42*, 4795. (b) Manimaran, B.; Rajendran, T.; Lu, Y. L.; Lee, G. H.; Peng, S. M.; Lu, K. L. *Eur. J. Inorg. Chem.* **2001**, *3*, 633. (c) Slone, R. V.; Hupp, J. T.; Stern, C. L.; Albrecht-Schmitt, T. E. *Inorg. Chem.* **1996**, *35*, 4096. (d) Saalfrank, R. W.; Reimann, U.; Goritz, M.; Hampel, E.; Scheurer, A.; Heinemann, F. W.; Busches, M.; Daub, J.; Schunemann, V.; Trautwein, A. X. *Chem. Eur. J.* **2002**, *8*, 3614. (e) Saalfrank, R. W.; Trummer, S.; Reimann, U.; Chowdhry, M. M.; Hampel, F.; Waldmann, O. *Angew. Chem., Int. Ed.* **2000**, *39*, 3492.

(7) (a) Das, N.; Mukherjee, P. S.; Arif, A. M.; Stang, P. J. *J. Am. Chem. Soc.* **2003**, *125*, 13950. (b) Mukherjee, P. S.; Das, N.; Kryshchenko, Y. K.; Arif, A. M.; Stang, P. J. *J. Am. Chem. Soc.* **2004**, *126*, 2464.

(8) (a) James, S. L. *Chem. Soc. Rev.* **2003**, *32*, 276. (b) Mukherjee, P. S.; Dalai, S.; Zangrando, E.; Lloret, F.; Chaudhuri, N. R. *Chem. Commun.* **2001**, 1444. (c) Konar, S.; Mukherjee, P. S.; Zangrando, E.; Lloret, F.; Chaudhuri, N. R. *Angew. Chem., Int. Ed.* **2002**, *41*, 1562.

(9) Caulder, D. L.; Raymond, K. N. *J. Chem. Soc., Dalton Trans.* **1999**, 1185.

Scheme 2. Schematic Presentation of the Formation of Dimanganese (**3a**) and Tetrazinc (**3b**) Products^a**Figure 1.** ORTEP view of complex **3a** with atom numbering scheme (thermal ellipsoids are drawn at 30% probability level).

a axis analogous to that observed in the neutral Pt rectangles.^{7b} The intermolecular Mn–Mn distance along the *a* axis is 12.7 Å.

Crystal Structure of Complex 3b. The crystal structure of **3b** indicates that this complex is a discrete tetrazinc neutral product with both tetrahedral and octahedral Zn-centers (Figure 3). This structure consists of a Zn₄(OAc)₆(OH)₂ motif and two bridging ligands **1**. One pyridine moiety of each ligand is coordinated to the tetrahedral zinc while the other is coordinated to an octahedral metal center. Four of the acetates behave as bidentate bridging ligands and bridge both the tetrahedral and the octahedral zinc. The remaining two acetates are monodentate and are coordinated to the octahedral zinc centers. Each μ₃-OH is coordinated to two octahedral zincs and one tetrahedral zinc. The Zn(1)–Zn(2) separation is 3.45 Å which is shorter than the Mn–Mn separation in **3a**, indicating that the clip is more compressed

in the center and thus **3b** is potentially more strained compared to **3a**. Selected bond lengths and angles around the coordination sphere of the metal centers are given in Table 2. No channel structure was found in this complex.

Magnetic Properties of Complex 3a. The magnetic susceptibility, χ , of **3a** was investigated between 4 and 300 K. The room temperature effective magnetic moment μ_{eff} [$= (8\chi_{\text{MT}})^{1/2}$] is 5.91 μ_{B}/Mn in accord with the expectation of 5.92 μ_{B}/Mn indicative of isolated spin sites at room temperature. $\mu_{\text{eff}}(T)$ decreases with decreasing temperature (Figure 4) consistent with the presence of a weak antiferromagnetic interaction between the Mn(II) ions. These data were fit to an $S = 5/2$ dinuclear spin model (eq 1) (with N , β , and k being Avogadro's number, Bohr magneton, and the Boltzmann constant respectively, and $\theta =$ Weiss constant) based on the Hamiltonian $H = -2JS_1 \cdot S_2$ ($S_1 = S_2 = 5/2$).^{10a} The data can be fit with $J = -1.6(0.01) \text{ cm}^{-1}$ and $\theta =$

Table 1. Crystal Data and Structure Refinement for Complexes **3a** and **3b**

	3a	3b
empirical formula	C ₆₄ H ₄₄ Mn ₂ N ₄ O ₈	C ₆₈ H ₅₂ N ₄ O ₁₄ Zn ₄
fw	1106.91	1410.62
T/K	150(1) K	150(1) K
space group	<i>P</i> $\bar{1}$	<i>P</i> $\bar{1}$
<i>a</i> /Å	12.720(5)	9.5817(3)
<i>b</i> /Å	14.182(5)	12.725(3)
<i>c</i> /Å	15.589(4)	12.952(5)
α /deg	103.51(19)	95.881(18)
β /deg	91.115(20)	106.65(13)
γ /deg	109.13(16)	100.08(17)
<i>V</i> /Å ³	2569.23(15)	1470.11(8)
<i>Z</i>	2	1
μ (Mo K α)/mm ⁻¹	0.556	1.686
λ /Å	0.71073	0.71073
<i>R</i> _w ^a	0.1324	0.0834
<i>R</i> ^a	0.039	0.0369
<i>D</i> /Mg m ⁻³	1.431	1.593

$$^a R = \sum ||F_o| - |F_c|| / \sum |F_o|; R_w = [\sum \{w(F_o^2 - F_c^2)^2\} / \sum \{w(F_o^2)^2\}]^{1/2}.$$

−10.46(0.04) K. This is comparable to −1.6 cm⁻¹ for Mn^{II}₃(μ -O₂CCH₂Cl)₆(bipy)₂, a related manganese(II) complex with an acetate bridge.^{10b} Due to the long superexchange pathway, the coupling through **1** is negligible. The Weiss constant was calculated [$\theta = -10.34(0.23)$ K, $C = 9.11(0.01)$ cm³ mol⁻¹ K] from χ_M^{-1} versus *T* data (insert of Figure 4) using the Curie–Weiss equation.

$$H = -2JS_1 \cdot S_2 \text{ where } S_1 = S_2 = 5/2$$

$$\chi_M = \frac{N\beta^2 g^2}{3k(T - \theta)} \{ [6 \exp(2J/T) + 30 \exp(6J/T) + 84 \exp(12J/T) + 180 \exp(20J/T) + 330 \exp(30J/T)] / [1 + 3 \exp(2J/T) + 5 \exp(6J/T) + 7 \exp(12J/T) + 9 \exp(20J/T) + 11 \exp(30J/T)] \} \quad (1)$$

UV Properties of 3b. Upon formation, complex **3b** assumes an intense yellow color. The absorption spectrum of this complex is shown in Figure 5. The absorbance in the electronic spectrum exhibits a near-UV transition. The absorbance per building block **1** increases upon formation of **3b**; specifically, the anthracene-based absorbance, centered at 260 nm, increases significantly. In other words, the UV absorption of the ensemble **3b** is enhanced and greater than the absorbance of the sum of the building blocks. In contrast, the cationic assemblies showed a decrease in anthracene-based absorbance upon complex formation.^{3b}

Conclusion

The rigid organic clip **1**, composed of an anthracene moiety bearing two pyridines as monodentate coordination sites, in the presence of neutral metal acetates (metal = Mn and Zn) in a ratio of 1:1, leads to neutral dimanganese and tetrazinc molecules, respectively. In the crystal structure of

the manganese analogue, the rectangular units are packed in a parallel fashion along the *a* axis to form a channel structure not occupied by solvent molecules. Despite its ability to form oligomeric products by varying its bonding nature, ligand **1** prefers to form closed discrete products in its intermediates with Mn and Zn acetates.

Experimental Section

Methods and Materials. Acetate salts of manganese(II) and zinc(II) as hydrated forms were purchased from Aldrich and used as received. 1,8-Bis(4-pyridylethynyl)anthracene (**1**) was synthesized as previously reported.^{10c} Elemental analyses were performed by Atlantic Microlab, Norcross, GA. Magnetic data were collected on a Quantum Design MPMS-5XL 5 T SQUID magnetometer. UV–Vis spectra were recorded on a Hewlett-Packard 8452A spectrophotometer. IR spectra were recorded on a Nicolet 520 FTIR spectrometer in KBr pellets. NMR spectra were recorded on a Varian Unity 300 spectrometer. ¹H chemical shifts are reported relative to the residual protons of deuterated dichloromethane (δ 5.32 ppm). Mass spectra were obtained with a Finnigan MAT 8230 instrument.

X-ray Data Collection, Structure Solution, and Refinement.

A single crystal of the corresponding complex (**3a** or **3b**) was selected from the reaction product and was mounted on a glass fiber with traces of viscous oil and then transferred to a Nonius KappaCCD diffractometer equipped with Mo K α radiation ($\lambda = 0.71073$ Å). Ten frames of data were collected at 150(1) K with an oscillation range of 1 deg/frame and an exposure time of 20 s/frame.¹¹ Indexing and unit cell refinement were based on all observed reflections from those 10 frames. The structures were solved by a combination of direct methods using SIR 97.¹² Hydrogen atoms were assigned isotropic displacement coefficient $U(H) = 1.2U(C)$, and their coordinates were allowed to ride on their respective carbon using SHELXL97.¹³ All of the non-hydrogen atoms were refined with anisotropic displacement coefficients. Scattering factors were taken from the International Table of Crystallography, Vol. C.^{14,15} The weighting scheme employed was $w = 1/[\sigma^2(F_o^2) + (0.0253P)^2 + 18.4225P]$ where $P = (F_o^2 + 2F_c^2)/3$. The structure of **3a** showed disordered bridging acetates and hence a relatively high *R* factor. Details of the data collection, structure solution, and refinement are given in Table 1.

Preparation of Complex 3a. To a 5 mL dichloromethane solution containing 38.0 mg (0.10 mmol) of linker **1** was added a methanol solution (5 mL) of Mn(OAc)₂·4H₂O (0.10 mmol) drop-by-drop with continuous stirring. The resulting microcrystalline light yellow product (**3a**), which precipitated after 15 min stirring, was filtered and washed with methanol. Single crystals suitable for X-ray diffraction were grown by slow evaporation (over a week) of a dichloromethane solution of the product. Yield: 91%. Anal. Calcd

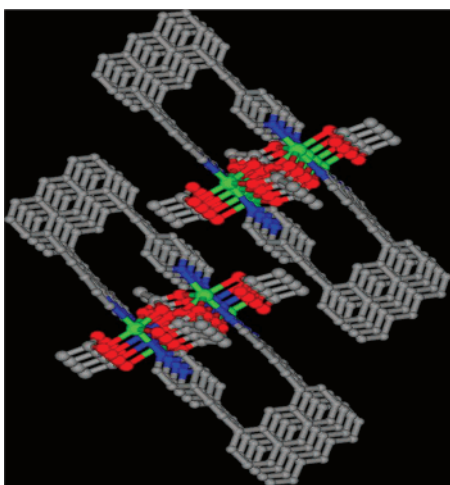
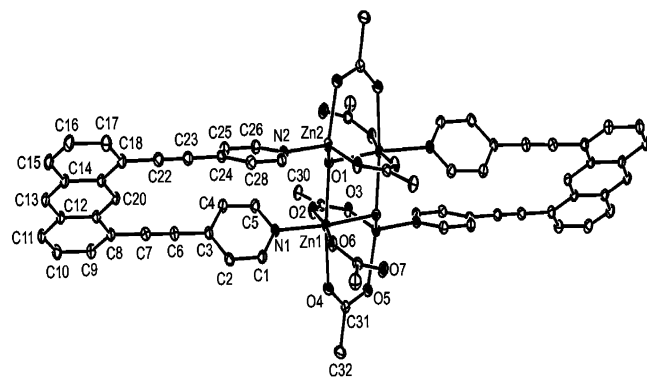
(10) (a) O'Connor, C. J. *Prog. Inorg. Chem.* **1982**, 29, 203. (b) Fernández, G.; Corbella, M.; Mahiya, J.; Maestro, M. A. *Eur. J. Inorg. Chem.* **2002**, 2502. (c) Kryschenko, Y. K.; Seidel, S. R.; Muddiman, D. C.; Nepomuceno, A. I.; Stang, P. J. *J. Am. Chem. Soc.* **2003**, 125, 9647.

(11) Nonius, B.V. *COLLECT Data Collection Software*, 1998.
 (12) Altomare, A.; Burla, M. C.; Camalli, M.; Cascarano, G.; Giacovazzo, C.; Guagliardi, A.; Moliterni, A. G. G.; Polidori, G.; Spagna, R. *SIR-97(Release 1.02)—A program for automatic solution and refinement of crystal structure*.
 (13) Sheldrick, G. M. *SHELX97 [Includes SHELXS97, SHELXL97, CIFT-AB] Programs for Crystal Structure Analysis (Release 97-2)*; University of Göttingen: Göttingen, Germany, 1997.
 (14) Maslen, E. N.; Fox, A. G.; O'Keefe, M. A. *International Tables for Crystallography: Mathematical, Physical and Chemical Tables*; Wilson, A. J. C., Ed.; Kluwer: Dordrecht, The Netherlands, 1992; Vol. C, Chapter 6, pp 476–516.
 (15) Creagh, D. C.; McAuley, W. J. *International Tables for Crystallography: Mathematical, Physical and Chemical Tables*; Wilson, A. J. C., Ed.; Kluwer: Dordrecht, The Netherlands, 1992; Vol. C, Chapter 4, pp 206–222.

Table 2. Selected Bond Lengths (Å) and Angles (deg) of Complexes **3a** and **3b**

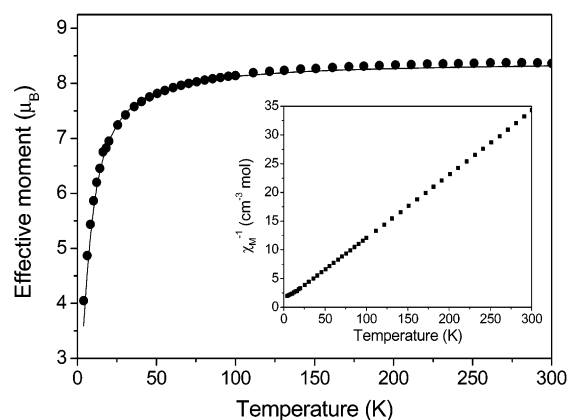
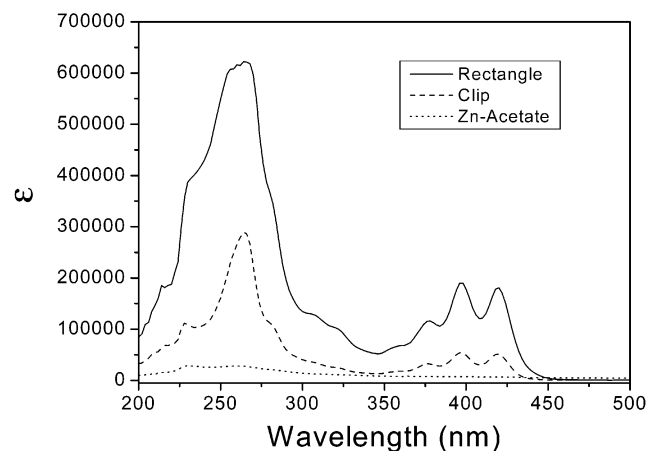
3a					
Mn(1)–N(1)	2.255(3)	Mn(1)–N(3)	2.263(3)	Mn(1)–O(3)	2.279(3)
Mn(1)–O(2)	2.294(3)	Mn(1)–O(5)	2.143(3)	Mn(1)–O(1)	2.279(3)
Mn(2)–O(4)	2.107(3)	Mn(2)–O(6)	2.155(3)	Mn(2)–O(1)	2.242(8)
Mn(2)–O(7)	2.290(3)	Mn(2)–N(2)	2.298(3)	Mn(2)–N(4)	2.278(3)
O(5)–Mn(1)–N(1)	96.78(15)	O(5)–Mn(1)–N(3)	94.45(15)		
N(1)–Mn(1)–N(3)	166.6(12)	O(5)–Mn(1)–O(1)	138.1(12)		
N(1)–Mn(1)–O(1)	89.77(11)	N(3)–Mn(1)–O(1)	84.79(11)		
3b					
Zn(1)–O(6)	2.033(18)	Zn(1)–O(1)	2.066(17)	Zn(1)–O(4)	2.120(18)
Zn(1)–O(2)	2.165(19)	Zn(1)–N(1)	2.166(19)	Zn(2)–O(1)	1.909(17)
Zn(2)–N(2)	2.039(17)	O(3)–Zn(2)#1	1.961(19)	O(5)–Zn(2) ^a	1.993(17)
O(6)–Zn(1)–O(1)	90.03(7)	O(6)–Zn(1)–O(4)	92.01(8)		
O(1)–Zn(1)–O(4)	173.3(6)	O(6)–Zn(1)–O(2)	172.2(7)		
O(1)–Zn(1)–O(2)	93.28(7)	O(4)–Zn(1)–O(2)	85.50(8)		
O(6)–Zn(1)–N(1)	88.61(7)	O(1)–Zn(1)–N(1)	95.06(7)		
O(4)–Zn(1)–N(1)	91.33(7)	O(2)–Zn(1)–N(1)	84.03(7)		

^a $-x, -y + 1, -z + 2$.


Figure 2. Packing diagram of **3a** along the crystallographic *a* axis.

Figure 3. ORTEP view of complex **3b** with atom numbering scheme (thermal ellipsoids are drawn at 30% probability).

for $C_{64}H_{44}Mn_2N_4O_8$: C, 69.3; H, 3.97; N, 5.06. Found: C, 69.5; H, 4.21; N, 5.22. IR: $\nu(\text{COO}^-)$, 1617, 1561 cm^{-1} ; $\nu(\mu\text{-COO}^-)$, 1415 cm^{-1} ; $\nu(\text{C}\equiv\text{C})$, 2212 cm^{-1} . EI-MS: m/z : 1107.4 [M^+].

Preparation of Complex 3b. To a 5 mL dichloromethane solution containing 38.0 mg (0.10 mmol) of linker **1** was added a methanol solution (5 mL) of $\text{Zn}(\text{OAc})_2 \cdot 4\text{H}_2\text{O}$ (0.10 mmol) drop-by-drop with continuous stirring. The resulting intense yellow solution was filtered after stirring 2 h to remove the impurities. Overnight diffusion of diethyl ether into the filtrate resulted in


Figure 4. Fitting of effective magnetic moment versus temperature (K) data using dimer model of $S = 5/2$ local spin. Solid line shows the best fit obtained.

Figure 5. Absorption spectra of **3b** (20 μM) and building blocks **1** (40 μM) and Zn(II)-acetate (80 μM).

yellow prismatic single crystals suitable for X-ray diffraction. Yield: 83%. Anal. Calcd for $C_{68}H_{52}N_4O_{14}Zn_4$: C, 57.9; H, 3.68; N, 3.96. Found: C, 58.3; H, 3.91; N, 3.72. IR: $\nu(\text{COO}^-)$, 1611, 1568 cm^{-1} ; $\nu(\mu\text{-COO}^-)$, 1422 cm^{-1} ; $\nu(\text{C}\equiv\text{C})$, 2214 cm^{-1} ; $\nu(\text{O-H})$, 3144 cm^{-1} . EI-MS: m/z : 1380.1 [$M^+ - C_2H_6$]. ^1H NMR (CD_2Cl_2): δ 9.51 (s, 2H, H_9); 8.60 (s, 2H, H_{10}); 8.16 (d, 8H, H-py); 7.91 (d, 8H, H-py); 7.56 (m, 12H); 1.62 (s, 18H, H-Me); 1.25 (s, 2H, $\mu\text{-OH}$).

Preparation of Complex 4. This complex was prepared using the method described for **3a** and **3b** upon reaction of $\text{Cu}_2(\text{CH}_3\text{-COO})_4 \cdot 2\text{H}_2\text{O}$ (0.10 mmol) and **1** (0.10 mmol). The resulting green precipitate was filtered after stirring 1 h. Yield: 77%. Anal. Calcd for $\text{C}_{32}\text{H}_{22}\text{CuN}_2\text{O}_4$: C, 68.3; H, 3.91; N, 4.98. Found: C, 69.1; H, 4.11; N, 5.20. IR: $\nu(\text{COO}^-)$, 1614, 1563 cm^{-1} ; $\nu(\text{C}\equiv\text{C})$, 2213 cm^{-1} .

Acknowledgment. Financial support from the National Science Foundation (CHE-0306720) and the Department of

Energy Division of Materials Science (Grant DE-FG03-93ER45504) is gratefully acknowledged.

Supporting Information Available: Crystallographic data for **3a** and **3b** in CIF format. Additional tables of crystallographic data in PDF format. This material is available free of charge via the Internet at <http://pubs.acs.org>.

IC0493088